Contents lists available at http://qu.edu.iq

Al-Qadisiyah Journal for Engineering Sciences

Journal homepage: https://qjes.qu.edu.iq

Control of self-excited induction generator based wind turbine using current and voltage control approaches

S. Ratheesh * ***and Jeba Vins M.***

Sea Sense Interdisciplinary Research and IT Solutions OPC Pvt Ltd., Marthandam, Kanyakumari, Tamil Nadu, 629165, India

ARTICLE INFO

Article history:
Received 02 July 2023
Received in revised form 22 August 2023
Accepted 29 September 2023

Keywords:
Fuzzy-based
Generator
Converter
Wind Turbine
Current-Voltage

ABSTRACT

The self-excited induction generator (SEIG) is widely applied in the wind energy conversion system (WECS) to enhance power generation. The power generation from WECS is varied in terms of varying wind speed. Hence, to improve the working of SEIG-based WECS, the multi-stage coati optimized proportional integral (CPI) fractional order proportional integral derivative (FOPID) controller is proposed in this work. The proposed coati optimized proportional integral - fractional order proportional integral derivative controls the SEIG's grid side converter and generator side converter. The coati optimization algorithm optimizes the controller parameters of a proposed multi-state controller. The proposed CPI-FOPID controls both the voltage at the grid side converter and the current at a generator side converter. Moreover, the pitch angle of the wind turbine (WT) is controlled by the fuzzy-based tilt integral derivative (F-TID) controller. The proposed work will be implemented on the Matlab/Simulink platform, and the THD of 0.63% has proven the efficacy of the proposed methodology.

1. Introduction

The steadily rising demand for energy is causing the fast depletion of fossil fuels like coal and oil. Thus, several efforts are taken technically and economically to lessen the usage of fossil fuels for power generation [1]. Thus, renewable energy sources (RES) based energy generation technology is developed in the energy market. Several countries around the globe are using RES-based energy generation to enlarge the installed capacity of power generation units [2]. The RES is partly complex and has an inherent complex nature, which affects the system reliability and available power generation at a certain condition [3]. One of the rapidly growing and steadily available RES technologies is the wind energy conversion system (WECS). In the wind energy conversion system, induction machines transform the wind's kinetic energy into power [4]. The WECS comprises components like an aerodynamic rotor, a power electronic interface, and generators. All these components are connected to the grid through the transmission line. Among these devices, the generator is considered a vital piece of equipment that plays an important role in system stability [5]. Over the years, generator types such as synchronous and asynchronous generators have been adopted with the wind turbine (WT). The selection of generators in WECS is a complicated task, especially in grid-integrated power systems. Different configurations of WECS are fixed speed (FS), variable speed (VS), doubly fed induction generator (DFIG), and full VS types [6]. The self-excited induction generator (SEIG) is popular among several types of induction machines owing to its protection against short circuits and reduced maintenance cost [7, 8]. The SEIG is well known for

* *Corresponding author.*
E-mail address: sratheeshtpm@gmail.com (S. Ratheesh)

https://doi.org/10.30772/qjes.2023.143509.1033

its cheaper cost and better performance [9]. The SEIG-based WT compensates for the network's reactive power through the capacitor banks. Voltage instability is a critical factor in the WT-connected power system. Voltage stability indicates the system's ability to withstand after being subjected to a fault. However, the voltage stability can be improved by minimizing the amount of reactive power delivered to the system. Due to the continuous operation of WT, the voltage and current limits may experience violations [10, 11]. The prime objective of control strategies in WT is to ensure stable operation during grid integration and deliver constant power to the grid. Controlling actions are improved by adding an effective method for torque and pitch angle control [12]. In [13], a fuzzy-based control technique was used to enhance the converter operation of standalone WT. Pitch angle control to the WT can be provided using a sliding mode controller and adaptive gain [14]. However, power quality (PQ) and stability become important considerations in wind power plants.

The PQ issues can be compensated by controlling the voltage and current in the system. However, the voltage and current regulation in the SEIG is affected by the excitation capacitance and variations in speed [15]. Moreover, the performance of SEIG is affected by the impedance load and loss of residual mechanism depending on the voltage and frequency [16]. The output frequency of the generator has a great impact on the speed of WT; thus, it is necessary to control the speed of the turbine. Furthermore, the speed of a turbine is adjusted by controlling the pitch angle. An efficient control architecture of the controller will enhance efficiency [17].

In some cases, the maximum power point tracking (MPPT) algorithm that drives the operating points near optimality can accomplish voltage control in SEIG. In the MPPT controller-based approaches, the turbine speed increases so that the system will provide higher power [18]. The most popular approach in SEIG-based WT is the fuzzy logic (FL))-based controllers. The FL-based approaches require plant knowledge to generate the membership functions [19, 20]. The proportional-integral (PI) controller is adopted in the system to cater to these issues. The major drawback of this PI is the variations of control gains due to uncertainties in the system. Hence, the optimized controllers are preferred to provide optimum speed and voltage control.

The reference frame theory reduces the complexities in SEIG control models. Thus, the proposed controller adopts transformation theories to obtain the desired operation of the induction generator. The optimized proportional integral derivative (PID) controller is used in this work to achieve the optimum operation of SEIG-based WT. The major contributions of this work are given as,

- Improve the voltage control on the grid side converter using a coati-optimized multi-stage controller.
- Enhance the current control on the generator side converter using the CPI-FOPID controller.
- Improve the pitch angle control using a fuzzy-based tilt integral derivative (F-TID) controller.

The paper is structured as follows; Section 2 discusses various kinds of literature. The proposed control strategy is elaborated in Section 3. Results are added in Section 4, and a conclusion is given in Section 5.

2. Related Works

Several controllers used in SEIG-based WT are discussed in this section.

Reddy et al. [21] introduced an ANFIS controller for the inverter in SEIG attached wind power plant. Dynamic vector control was used in the machine reference model. The ANFIS controller controlled the voltage in that suggested model, and a turbine's pitch angle controlled frequency. In that suggested model, the ANFIS controller had an output-layer neuron. The wind turbine's power coefficient determines the blade angle in the turbine model.

Angadi et al. [22] suggested a maximum power point tracking methodology for the wind turbine to power the induction motor pump. The optimization-based power maximizing methodology generates appropriate switching pulses to the converter model. That suggested model was sensorless and could generate the switching pulses based on the operating frequency of the voltage source converter. The current in the SEIG and DC link was fed into the controller, which provides controlled switching pulses to the inverter. In this way, the power output can be maximized in the inverter. Sotoudeh et al. [23] suggested two control architectures for the machine-side and grid-side converters. The machine-side controller keeps the electromagnetic flux at a limited value to maintain the electromagnetic torque. In this process, the resistor value of the stator was obtained by an estimator, and the new reference was estimated using a PI controller. The controller on the machine side was designed based on the linearization method. The estimator evaluates the resistance of the stator at different moments. Moreover, the grid-side controller regulates reactive and active power flow to the grid. The grid-side controller was designed based on a sliding mode control strategy.

Dagang et al. [24] introduced the fuzzy-based controlling architecture for the converters on the grid side. In that suggested model, the direct fuzzy control laws were updated to extract maximum power from the system. In that suggested model, the torque and angle of the wind turbine were fed into the fuzzy controller that generates appropriate switching signals to the converter. The active and reactive power from the AC bus was fed to the fuzzy controller to tune the inverter operation.

Laghridat et al. [25] have suggested a control technology for rejecting the disturbance in the SEIG-based wind power plant. That suggested model provided controlled active and reactive power through induction generators and back-to-back converters. A distribution algorithm and wind turbines were also used to provide wind farm power. Moreover, the maximum power tracking control was used to extract the peak power from the wind turbine. The transmission system operator controlled the active and reactive power flow. That suggested method was implemented at three power plants connected to wind turbines. Emami et al. [26] introduced a fault current limiter for reducing the sub-synchronous resonance of the wind farm. The suggested model was investigated on the power system containing 2 wind turbines. The short circuit current in wind power plants was minimized through the current limiter. That suggested model was investigated under different fault conditions. During the faulty condition, the fault current gets increased, and the current limiter will reduce the impacts of current in the model by minimizing the inductance limit.

Hamoodi et al. [27] introduced a fuzzy-based PID for controlling the pitch angle of SEIG-based WT. The pitch actuator regulates the rotation of WT with its horizontal axis, where the fuzzy logic was applied for selecting optimum values for the PID. In the suggested model, the reference and measured value of the pitch angles were entered into the controller. Meanwhile, the fuzzy logic examines both pitch angle error and error deviations. In this way, the fuzzy rules choose the optimum parameters of the PID. This method suggests that the tuned PID efficiently improved the system's stability.

3. Proposed Methodology

The PID controller is widely used in several applications due to its simple structure, low cost, and ease of implementation. At the same time, properly

tuning the controller will improve the desired performance. In this proposed work, the CPI-FOPID controller controls the SEIG-based WT. The proposed C-PID regulates the current in the generator side converter and the voltage in the grid side converter. The controlling architecture of a proposed methodology is shown in Fig. 1. The architecture shows that a step-up gearbox connects the SEIG to the turbine.

Moreover, the fixed capacitor is connected in parallel with a generator. The induction generator is started with the aid of fixed capacitor banks. The power generated from SEIG is fed into the rectifier to convert the variable voltage to rectified DC voltage. Afterward, the multi-level inverter is connected to minimize the switching frequency and voltage stress on the switches. The grid and generator side converter control strategies are carried out through the park and Clarke transformations.

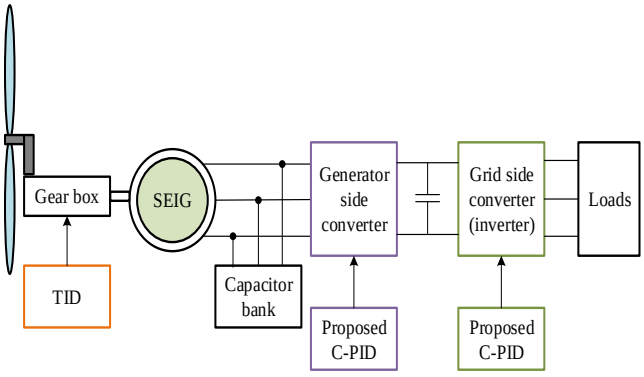

Figure 1: Proposed methodology

3.1 Modelling of SEIG-based WT

The WECS comprises components like a rotor, gearbox, generator, and WT. In the SEIG-based WECS, the generator is connected to the WT through the gearbox. The induction generator is connected to the capacitor bank for self-excitation. In such a system, the power is generated by converting the kinetic energy produced by the blade into electrical energy through SEIG. The kinetic energy produced by the WT is expressed in the Eq.1.

$$E_k = \frac{1}{2} \times v^2 \times \varpi \quad (1)$$

Here, v is the wind velocity, and ϖ is the mass of a blade. The following equation examines the tip speed ratio, Eq.2.

$$\lambda = \frac{\omega \times r}{v} \quad (2)$$

Here, ω and r are the angular speed of the blade and radius, respectively. The following equation examines the mechanical torque generated in the WT.

$$T = C \times \omega^2 \quad (3)$$

Here, C is the power coefficient. The modeling equations of SEIG in a d-q reference frame using the following equations.

$$V_{cq} = \frac{1}{C} \int i_{qs}\, dt + V_{cq0} \quad (4)$$

$$V_{cd} = \frac{1}{C} \int i_{ds}\, dt + V_{cd0} \quad (5)$$

Here, V_{cq} and V_{cd} are the capacitor voltages in q and d frames, respectively, i_{qs} and i_{ds} are the current in the direct axis and quadrature axis, respectively. The rotor flux linkages in both the direct and quadrature axes are expressed as follows.

$$\kappa_{qr} = L_m i_{qs} + L_r i_{qs} + \kappa_{qr0} \quad (6)$$

$$\kappa_{dr} = L_m i_{ds} + L_r i_{ds} + \kappa_{dr0} \quad (7)$$

Here, κ_{qr} and κ_{dr} are flux linkages in the direct and quadrature axis, respectively, L_r is the rotor inductance [28, 29]. The schematic diagram of SEIG in the d-q frame is shown in Fig. 2.

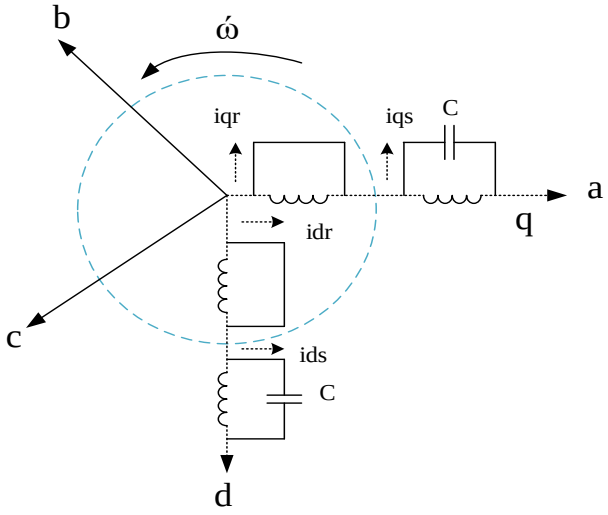

Figure 2: Representation of SEIG in d-q frame

The voltage and current measuring equations of the stator and rotor of SEIG are elaborated in [30]. The proposed control strategy for voltage and current control is explained further.

3.2 Working procedure of the proposed controllers

Park and Clarke's transformations are used in the control architecture to regulate the system's voltage and current. The Clarke transformation converts time domain components of the three-phase signals (ABC) into an orthogonal stationary frame (αβ) of two components. The park transforms two components into the rotating reference frame (d-q) [31]. The control architecture of the proposed control methodology is shown in Figure 3. As it is shown that the three-phase voltage at the grid side is measured, the Clarke transformation is carried out. Then the error in measured voltage is fed into the CPI-FOPID controller. Afterwards, the controlled voltage is given to the pulse width modulation strategy to produce optimum switching signals to the inverter. These steps are followed in the current control in the generator side converter. Moreover, the speed of WT is measured and fed into the F-TID controller. Finally, the controlled speed of the turbine is provided to the gearbox.

3.2.1 Voltage control using coati optimized multi-stage PI-FOPID controller

The controlling gains of controllers are improved by adding multi-stage controllers in the system. Hence, in this proposed work, the proportional-integral (PI), proportional derivative (PD), and fractional order proportional integral derivative (FOPID) are combined. The basic modeling equations of these controllers are shown below.

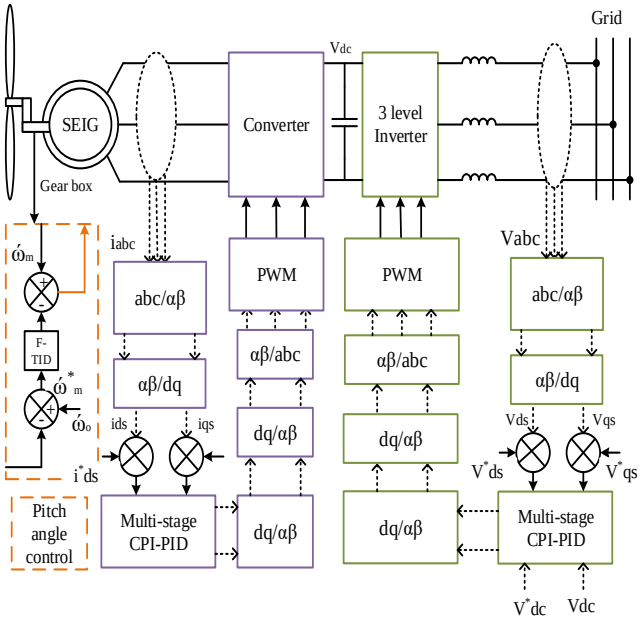

Figure 3: Proposed control architecture of SEIG-based WT

$$G_{pd}(s) = \kappa_p + \kappa_d \frac{d}{dt} e \quad (8)$$

$$G_{pi}(s) = \kappa_p + \kappa_i \int edt \quad (9)$$

$$G_{pid}(s) = \kappa_p + \kappa_i \int edt + \kappa_d \frac{d}{dt} e \quad (10)$$

$$G_{fopid}(s) = \kappa_p + \frac{\kappa_i}{s^{\lambda}} + \kappa_d s^{\mu} \quad (11)$$

Here, the subscripts represent corresponding controller outcomes, κ_p, κ_i and κ_d are proportional, integral, and derivative control gains, respectively, λ and μ are the order of integrator and differentiator, respectively [32].

The basic architecture of CPI-FOPID is shown in Figure 4. This proposed controller gives the error in Vdc and the d-q voltage errors. The first block controls the DC link voltage error provided into the COA. The objective function of the COA is to optimize the controlling parameters of the proportional derivative controller. Based on the optimized tuning of the P and D gains, the Vds Voltage is controlled. Then the PID controller is used to reduce Vqs voltage. Finally, the controlled voltage generates switching pulses to the inverter.

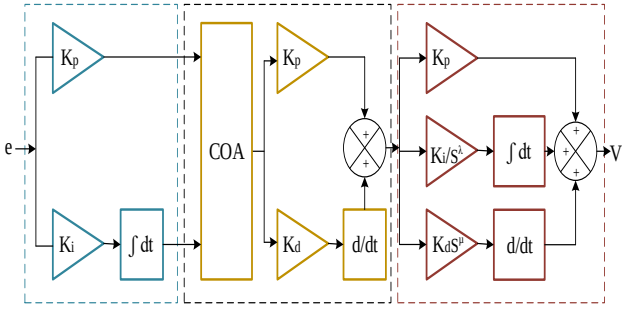

Figure 4: Proposed multi-stage CPI-FOPID controller

3.2.2 Proposed C-PID controller

The COA is developed based on coatis' natural hunting and confronting behaviors. This algorithm efficiently balances the exploration and exploitation phases [33].

- **Objective function**

The objective function ensures optimal control operations in the system. Regarding frequency control, the objective function of time integral multiplied by absolute error has provided superior performance. Based on this concern, the proposed work examines the ITAE as an objective function for the error minimization of control parameters.

$$Objective = ITAE = \int_0^T |\Delta V|\, tdt \rightleftarrows \quad (12)$$

Where ΔV is the voltage error, and T which is the simulation period.

The mathematical modelling of COA is given below, Eq. 13.

$$c_{m,n} = l_n + \lambda \rightleftarrows (u_n - l_n), m = 1,2,3\ldots in = 1,2,3\ldots j \quad (13)$$

Here, $c_{m,n}$ is the value of n^{th} decision variable, i is the total number of problem variables, j is the decision variable, λ is the random number [0, 1], l_n and u_n are lower and upper boundaries, respectively. The population matrix of the variables is shown in Eq. 14.

$$C = \begin{bmatrix} c_1 \\ c_m \\ c_N \end{bmatrix}_{j \times N} = \begin{bmatrix} c_{1,1} c_{1,n} c_{1,j} \\ c_{m,1} c_{m,n} c_{m,j} \\ c_{N,1} c_{N,n} c_{N,j} \end{bmatrix}_{j \times N} \quad (14)$$

The following Eq. 15 estimates the objective function of controlling parameters,

$$K = \begin{bmatrix} K_1 \\ K_m \\ K_N \end{bmatrix}_{j \times N} = \begin{bmatrix} K(c_1) \\ K(c_m) \\ K(c_N) \end{bmatrix}_{j \times N} \quad (15)$$

here K is the vector of the obtained objective function, K_m is the objective function of the corresponding parameter.

- **Phase 1:**

In this phase, the attacking behaviour of coati is used to calculate the best position. This work considers the best position as the optimum value of the control parameters. The position-varying Eq. 16 is expressed as follows:

$$c_{m,n}(p1) = c_{m,n} + \lambda(\gamma_g - \gamma_{c_{m,n}}) form = 1,2,\ldots \left[\frac{i}{2}\right], n = 1,2,\ldots j \quad (16)$$

The ground movement of coati is expressed in the following equation,

$$\gamma_n^g = l_n + \lambda \rightleftarrows (u_n - l_n), n = 1,2,\ldots i \quad (17)$$

The following equation is used for updating the solution, for $m = \left[\frac{1}{2}\right] + 1, \left[\frac{1}{2}\right] + 2, \ldots . N$ and $n = 1,2,\ldots . . i$.

$$c_{m,n}^{p1} = \begin{cases} c_{m,n} + \lambda\left(\gamma_n^g - \gamma . c_{m,n}\right), if F_g < F_m \\ c_{m,n} + \lambda\left(c_{m,n} - \gamma_n^g\right), else \end{cases} \quad (18)$$

$$c_m = \begin{cases} c_m^{p1}, if F_m^{p1} < F_m \\ c_m, else \end{cases} \quad (19)$$

here, c_m^{p1} is the updated values of m^{th} parameter, F_m^{p1} is the objective function, γ_n^g is an optimum range in the search space, γ is an integer in between [1, 2], F_g is the optimum range in the search space.

- **Phase-2**

The exploitation phase of COA is developed based on the escaping behaviour that is mathematically represented as Eqs. 20-22.

$$l_{bn}^{local} = \frac{l_{bn}}{t}, u_{bn}^{local} = \frac{l_{bn}}{t}, where, t = 1,2,\ldots T \quad (20)$$

$$c_{m,n}^{p2} = c_{m,n} + (1 - 2\lambda).\left(l_b^{local} + \lambda.\left(u_b^{local} - l_b^{local}\right)\right), i = 1,2,..N; j =$$

$$1,2,\dots i \tag{21}$$

$$c_m = \begin{cases} c_m^{p2}, if F_m^{p2} < F_m \\ c_m, else \end{cases} \tag{22}$$

Here, c_m^{p2} is the new solution updated based on the second phase, u_b^{local} and l_b^{local} are the lower and upper boundaries of local search space, respectively. The flow of COA for optimum parameter tuning is shown in Fig. 5.

3.2.3 Frequency control using fuzzy-tuned TID

The system frequency will be controlled by controlling the pitch angle of WT. The fuzzy-based controller has proven superior performance in induction motor control applications [34]. The pitch angle control has a great impact on the power generation of a wind turbine. In the proposed control architecture, the reference and measured speed of the turbine are fed into the F-TID controllers. Based on the error parameters, the fuzzy logic generates the control gains for the TID controller. The controller block of a proposed F-TID-based pitch angle control is shown in Figure 6. The fuzzy rules are shown in Table 1.

4. Results and Discussion

The proposed work is implemented on Matlab/Simulink tool, and the results regarding varying system conditions are taken. The results obtained from the proposed methodology are discussed in this section. The variation in excitation capacitance, terminal voltage, and current based on the load power is shown in Figure 7. It is shown that the excitation capacitance is increased with a higher load power value at synchronous speed. The results show that high power is obtained at 50µF excitation capacitance. Moreover, the terminal voltage is kept constant by adding more capacitance. It shows that the terminal voltage is 220V for the varying load power values.

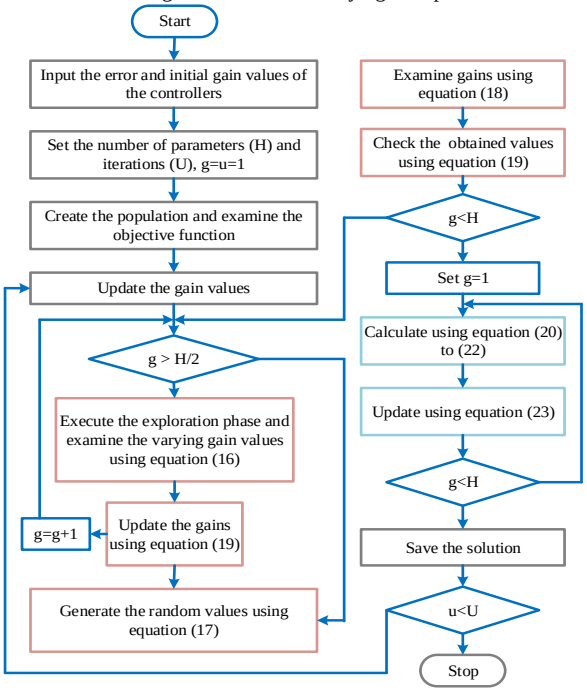

Figure 5: Flowchart of COA

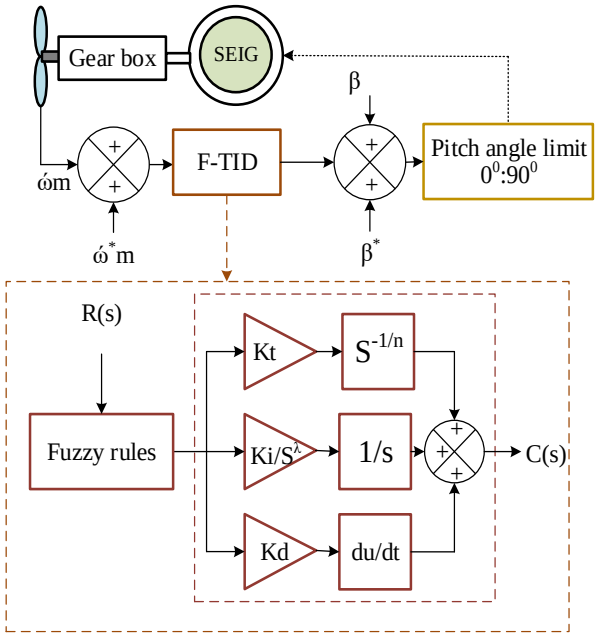

Figure 6: Pitch angle control using proposed F-TID

Table 1: Fuzzy rules

de / e	-	+	0
-	-	+	+
+	-	0	+
0	-	-	0

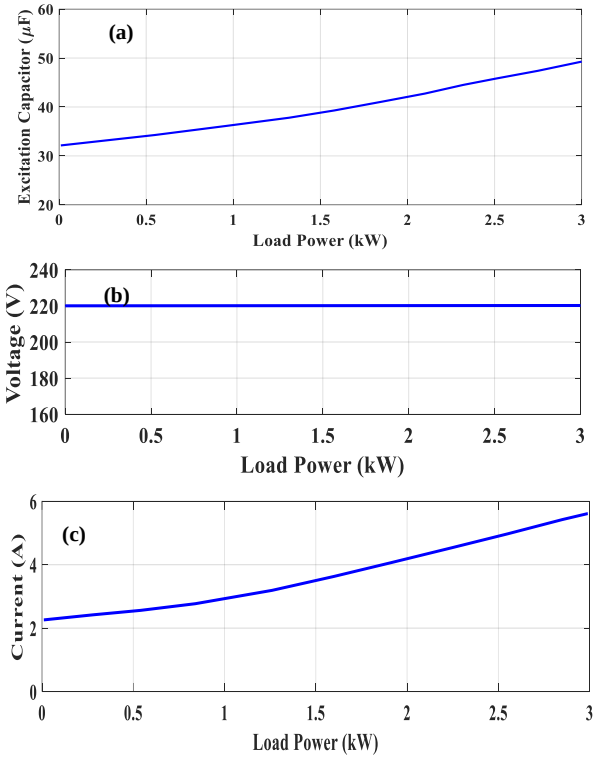

Figure 7: Load power for (a) Excitation capacitor, (b) Terminal voltage and (c) Current

The excitation capacitance for varying terminal voltage and stator current is shown in Figure 8. These results show the voltage increases with the lower excitation capacitance value. Moreover, the stator current increases with the higher excitation capacitance value under fixed speed.

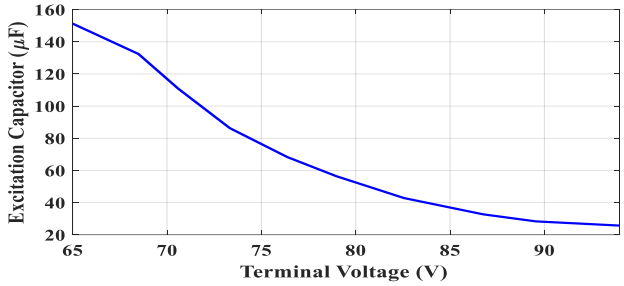

(a)

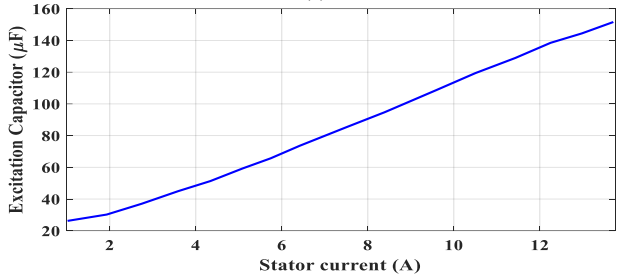

(b)

Figure 8: Excitation capacitance for (a) Terminal voltage and (b) Stator current at a fixed speed

- **Case 1:** System under normal condition

The results obtained from WECS under normal condition is shown in Figure 9. This proposed work gives the wind speed of 12m/s as input to the WECS. Based on this input, the proposed model provides 4KW power output, shown in Figure 9 (c). For this power, the reactive power measured is 1.3VAr.

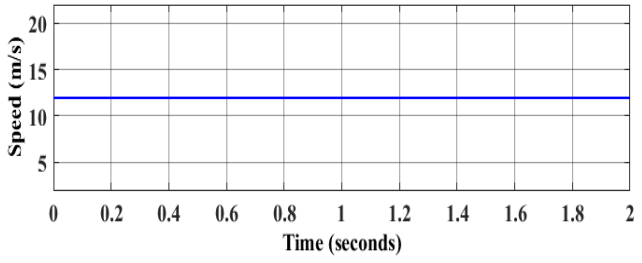

(a)

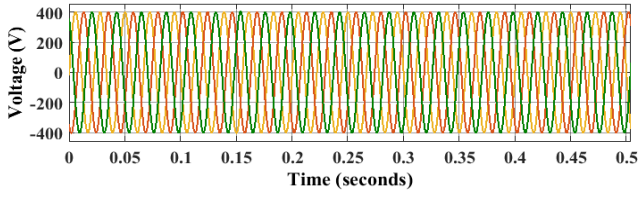

(b)

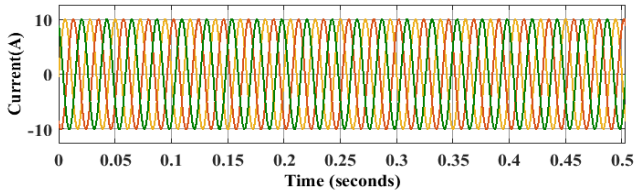

(c)

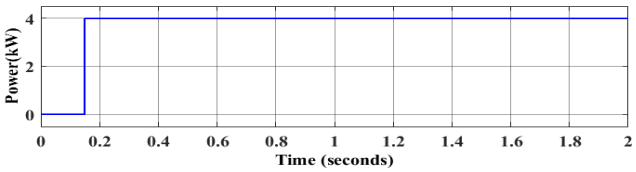

(d)

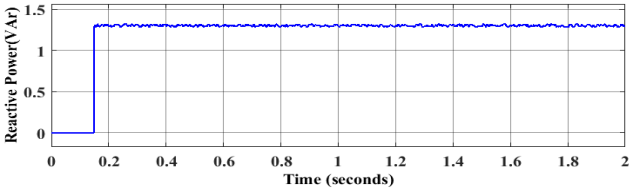

(e)

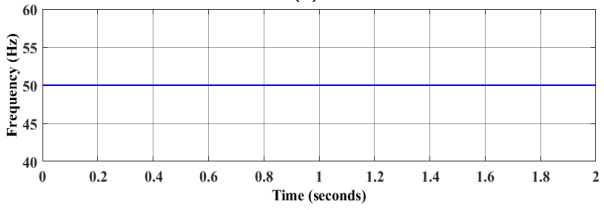

(f)

Figure 8: Results of the proposed model (a) Wind speed input (b) Voltage (c) Current (d) Power (e) Reactive power and (f) Frequency

- **Case-2:** Analysis of the system under the single line to ground (LG) fault

In this case, the fault is applied between 0.85s and 0.95s, and the corresponding results are shown in Figure 9. The current value in the single phase exceeds the nominal value during the faulty condition. Whereas the voltage in single-phase is reduced to zero in a faulty condition.

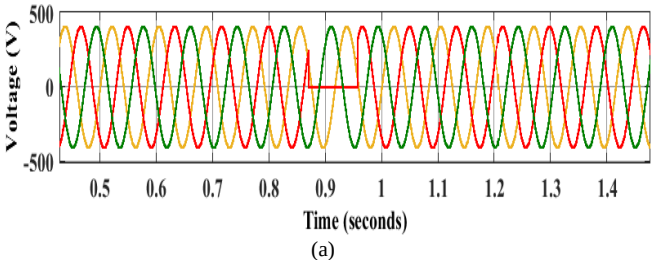

(a)

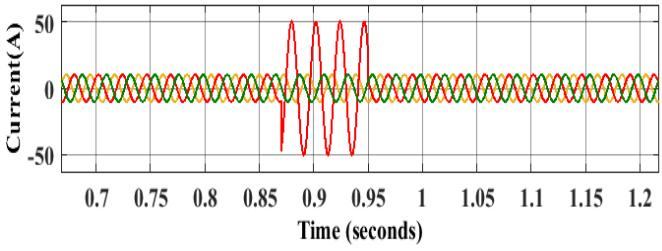

(b)

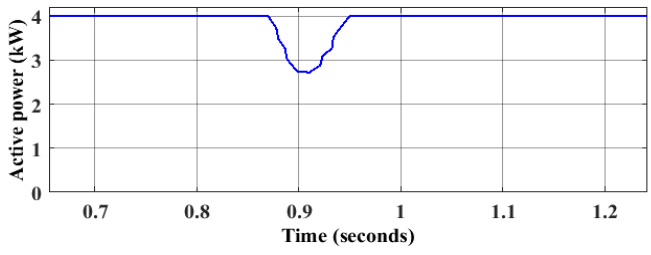

(c)

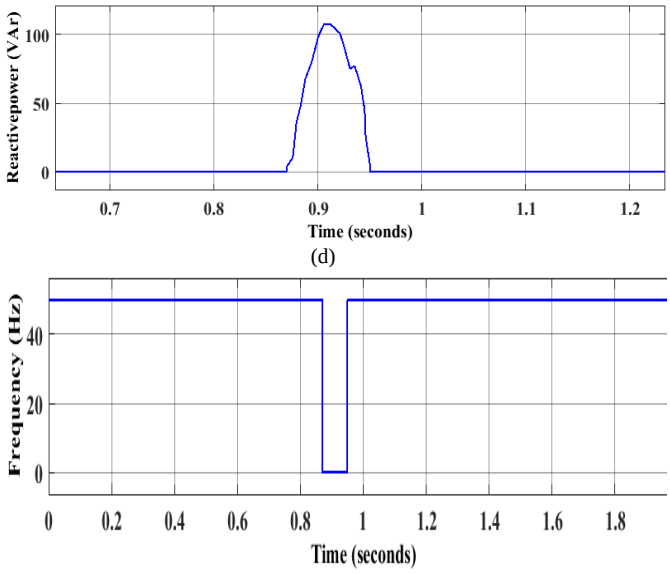

Figure 9: System under LG fault (a) Voltage (b) Current (c) Active power (d) Reactive power and (e) frequency

In this case, the LLG fault is applied between 0.85s and 0.95s, and the corresponding results are shown in Figure 10. The current value in two phases exceeds the nominal value during faulty conditions. At the same time, the voltage in the two phases was reduced to zero in a faulty condition.

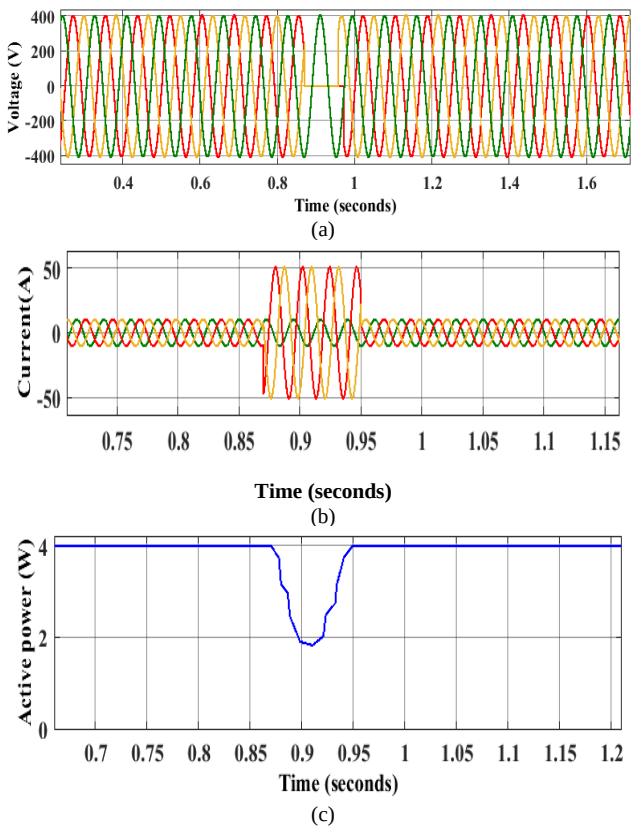

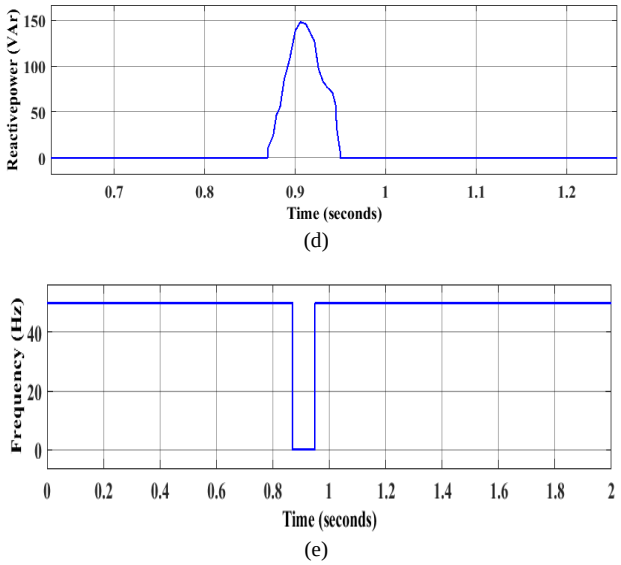

Figure 10: System under LLG fault (a) Voltage (b) Current (c) Active power (d) Reactive power and (e) frequency

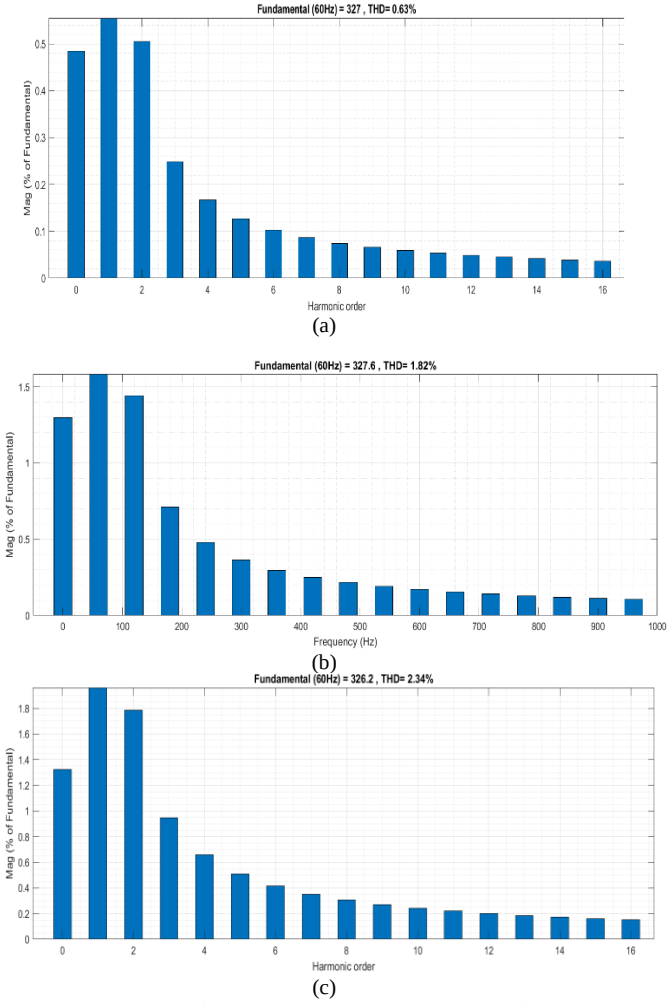

Figure 11: Analysis of THD (a) Normal condition, (b) LG fault condition and (c) LLG fault condition

4.1 Analysis of THD under different condition

This section has verified the THD of a proposed approach under different operating conditions. The THD of a suggested method under different operations is shown in Figure 11. It is shown that the proposed model has better THD under normal operating conditions compared with faulty conditions.

5. Conclusion

This paper has proposed a multi-stage CPI-FOPID controller to improve power generation at varying wind speed ranges. The proposed controller combines the PI, PD and FOPID controllers. The proposed CPI-FOPID not only controls the system voltage but also controls the current at the generator. The COA optimizes the controller gains based on the ITAE. Moreover, the pitch angle of WT is controlled by minimizing the speed error. The fuzzy logic controller optimizes the controlling gains of TID. The proposed controller with SEIG-WECS is implemented on Matlab/Simulink tool. Moreover, the results are verified in terms of varying ranges of speed. The results are verified by adding and removing the COA-based tuning. The comparative analysis shows that the proposed CPI-FOPID had improved the operation of SEIG-WECS irrespective of the speed variations. Moreover, the proposed method has provided a lower THD of 0.63% under normal operating conditions. Future work will be focused on improving the control of WECS under different load disturbances using an intelligent control approach.

Authors' contribution

All authors contributed equally to the preparation of this article.

Declaration of competing interest

The authors declare no conflicts of interest.

Funding source

This study didn't receive any specific funds.

REFERENCES

[1] J. Li, N.Wang, D. Zhou, W. Hu, Q. Huang, Z. Chen, F. Blaabjerg, Optimal reactive power dispatch of permanent magnet synchronous generator-based wind farm considering levelised production cost minimisation, Renewable Energy 145 (2020) 1-12.

[2] H.H. Kadhum, A.S. Alkhafaji, H.H. Emawi, The influence of iron losses on selecting the minimum excitation capacitance for self-excited induction generator (SEIG) with wind turbine, Indonesian Journal of Electrical Engineering and Computer Science 19(1) (2020) 11-22.

[3] F. Weschenfelder, G. Leite, DNP, ACA da Costa, O. de Castro Vilela, C.M. Ribeiro, A.A.V. Ochoa, A.M. Araujo, A review on the complementarity between grid-connected solar and wind power systems, Journal of Cleaner Production 257 (2020)120617

[4] F. Shahid, A. Zameer, A. Mehmood, M.A.Z. Raja, A novel wavenets long short term memory paradigm for wind power prediction, Applied Energy 269 (2020)115098

[5] B. Ramlochun, C.A. Vaithilingam, A.A. Alsakati, J. Alnasseir, Transient stability analysis of IEEE 9-bus system integrated with DFIG and SCIG based wind turbines, In Journal of Physics: Conference Series vol. 2120(1), (2021) 012023, IOP Publishing.

[6] IA de Azevedo, L.S. Barros, Comparison of control strategies for squirrel-cage induction generator-based wind energy conversion systems, In 2021 14th IEEE international conference on industry applications (INDUSCON) IEEE. (2021) 790-796.

[7] M.A. Haj-Ahmed, E.A. Feilat, H.I. Khasawneh, A.F. Abdelhadi, A.A. Awwad, Comprehensive protection schemes for different types of wind generators, IEEE Transactions on Industry Applications 54(3)(2018) 2051-2058.

[8] W. Na, E. Muljadi, S. Han, R.K. Tagayi, J. Kim, Possibility of power electronics-based control analysis of a self-excited induction generator (seig) for wind turbine and electrolyzer application, Electronics 10(22) (2021) 2743.

[9] R. Mahalakshmi, K.S. Thampatty, Analysis of SSR in Grid Integrated Series Compensated SCIG based Wind Turbine Generators-A Laboratory model, International Journal on Electrical Engineering and Informatics 13(2) (2021)336-353.

[10] A. Athamneh, AL-MAJALI BH. Voltage stability enhancement for large scale squirrel cage induction generator-based wind turbine using STATCOM, International Journal of Power Electronics and Drive Systems 12(3) (2021) 1784-1794.

[11] Y. Xu, T. Gao, Sub-synchronous frequency domain-equivalent modeling for wind farms based on rotor equivalent resistance characteristics, Global Energy Interconnection. 5(3) (2022) 293-300.

[12] O. Apata, DTO. Oyedokun, An overview of control techniques for wind turbine systems, Scientific African 10 (2020) e00566.

[13] S. Dewangan, G. Dyanamina, N. Kuma, Performance improvement of wind-driven self-excited induction generator using fuzzy logic controller, International Transactions on Electrical Energy Systems 29(8) (2019) e12039.

[14] A. Azizi, H. Nourisola, S. Shoja-Majidabad, Fault tolerant control of wind turbines with an adaptive output feedback sliding mode controller, Renewable energy 135 (2019) 55-65.

[15] K. Teng, Z. Lu, J. Long, Y. Wang, A.P. Roskilly, Voltage build-up analysis of self-excited induction generator with multi-timescale reduced-order model, IEEE Access 7 (2019)48003-48012.

[16] L. Varshney, A.S.S. Vardhan, A.S.S. Vardhan, S. Kumar, R.K. Saket, P. Sanjeevikumar, Performance characteristics and reliability assessment of self-excited induction generator for wind power generation, IET Renewable Power Generation 15(9) (2021) 1927-1942.

[17] BA. Nasir, R.W. Daoud, Modeling of wind turbine-self excited induction generator system with pitch angle and excitation capacitance control. In AIP Conference Proceedings 2307(1) (2020) 020022. AIP Publishing LLC.

[18] T. Amieur, D. Taibi, O. Amieur, Voltage oriented control of self-excited induction generator for wind energy system with MPPT, In AIP Conference Proceedings 1968(1) (2018) 030067. AIP Publishing LLC.

[19] J. Baran, A. Jąderko, An MPPT control of a PMSG-based WECS with disturbance compensation and wind speed estimation, Energies 13(23) (2020) 6344.

[20] K. Kim, H.G. Kim, Y. Song, I. Paek, Design and simulation of an LQR-PI control algorithm for medium wind turbine, Energies 2(12) (2019) 2248.

[21] S.R.K. Reddy, J.B.V. Subrahmanyam, A.S. Reddy, Improvement of Dynamic Performance in SEIG WECS by Using ANFIS Controller, Asian Journal for Convergence in Technology (AJCT) ISSN-2350-1146, 8(1) (2022) 78-86.

[22] S. Angadi, U.R. Yargatti, Y. Suresh, A.B. Raju, Speed sensorless maximum power point tracking technique for SEIG-based wind energy conversion system feeding induction motor pump. Electrical Engineering 104(5) (2022) 2935-2948.

[23] A. Sotoudeh, J. Soltani, M.M. Rezaei, A Robust Control for SCIG-Based Wind Energy Conversion Systems Based on Nonlinear Control Methods, Journal of Control, Automation and Electrical Systems 32, (2021) 735-746.

[24] CTS Dagang, G. Kenne, F.A. Muluh, Fuzzy logic direct torque/power control for a self-excited induction generator driven by a variable wind speed turbine, International Journal of Dynamics and Control 9 (2021) 1210-1222.

[25] H. Laghridat, A. Essadki, T. Nasser, Coordinated control by ADRC strategy for a wind farm based on SCIG considering low voltage ride-through capability, Protection and Control of Modern Power Systems 7(1) (2022) 7.

[26] Y. Emami, A. Koochaki, M. Radmehr, SSR Alleviation in SCIG-Based Wind Power Plants Using Resistive Bridge-Type FCL, Journal of Electrical Engineering & Technology 16(2) (2021) 907-916.

[27] S.A. Hamoodi, F.I. Hameed, A.N. Hamoodi, Pitch angle control of wind turbine using adaptive Fuzzy-PID controller, EAI Endorsed Transactions on Energy Web 7(28) (2020) e15-e15.

[28] O.S. Ejiofor, E.U. Candidus, M.C. Victory, E.C. Ugochukwu, Wind energy dynamics of the separately excited induction generator, International Journal of Applied Science. 2(1) (2019) 22-22.

[29] O.S. Ejiofor, E.U. Candidus, M.C. Victory, E.C. Ugochukwu, Wind energy dynamics of the separately excited induction generator, International Journal of Applied Science. Vol. 2(1), pp. 22-22, 2019.

[30] A.S. Farag, S.M. Saleh, G.M. El-Bayoumi, Pitch control dynamic study of isolated wind turbine based self-excited induction generator under realistic wind speed profiles, In 2017 Nineteenth International Middle East Power Systems Conference (MEPCON) (2017) 403-408. IEEE.

[31] A.S. Satpathy, D. Kastha, K. Kishore, Control of a STATCOM-assisted self-excited induction generator-based WECS feeding non-linear three-phase and single-phase loads, IET Power Electronics 12(4) (2019) 829-839.

[32] A. Singh, S. Suhag, Frequency regulation in an AC microgrid interconnected with thermal system employing multiverse-optimised fractional order-PID controller, International Journal of Sustainable Energy 39(3) (2020) 250-262.

[33] M. Dehghani, Z. Montazeri, E. Trojovská, P. Trojovský, Coati Optimization Algorithm: A new bio-inspired metaheuristic algorithm for solving optimization problems. Knowledge-Based Systems 259 (2023) 110011.

[34] NH. Mugheri, M.U. Keerio, An Optimal Fuzzy Logic-based PI Controller for the Speed Control of an Induction Motor using the V/F Method, Engineering, Technology & Applied Science Research 11(4) (2021) 7399-7404.